

1
2
3
4
5
6
7
8
9
10
11
12
13
14
15
16
17
18
19
20
21
22
23
24
25
26
27
28
29
30
31
32
33
34
35
36
37
38
39
40
41
42
43
44
45
46
47
48
49
50
51
52
53
54
55
56
57
58
59
60
61
62
63
64
65

1 **Title:** Monitoring in real time the cytotoxic effect of *Clostridium difficile* upon the
2 intestinal epithelial cell line HT29

4 **Authors:** Lorena Valdés, Miguel Gueimonde and Patricia Ruas-Madiedo*

6 **Affiliation:** Department of Microbiology and Biochemistry of Dairy Products. Instituto
7 de Productos Lácteos de Asturias – Consejo Superior de Investigaciones Científicas
8 (IPLA-CSIC).

10 * Corresponding author: IPLA-CSIC. Paseo Río Linares s/n, 33300 Villaviciosa,
11 Asturias, Spain. Tel: +34 98589213, Fax: +34 985892233; ruas-madiedo@ipla.csic.es

13 **Abstract**

14 The incidence and severity of *Clostridium difficile* infections (CDI) has been increased
15 not only among hospitalized patients, but also in healthy individuals traditionally
16 considered as low risk population. Current treatment of CDI involves the use of
17 antibiotics to eliminate the pathogen, although recurrent relapses have also been
18 reported. For this reason, the search of new antimicrobials is a very active area of
19 research. The strategy to use inhibitors of toxin's activity has however been less
20 explored in spite of being a promising option. In this regard, the lack of fast and reliable
21 *in vitro* screening methods to search for novel anti-toxin drugs has hampered this
22 approach. The aim of the current study was to develop a method to monitor in real time
23 the cytotoxicity of *C. difficile* upon the human colonocyte-like HT29 line, since
24 epithelial intestinal cells are the primary targets of the toxins. The label-free, impedance
25 based RCTA (real time cell analyser) technology was used to follow overtime the
26 behaviour of HT29 in response to *C. difficile* LMG21717 producing both A and B
27 toxins. Results obtained showed that the selection of the medium to grow the pathogen
28 had a great influence in obtaining toxigenic supernatants, given that some culture media
29 avoided the release of the toxins. A cytotoxic dose- and time-dependent effect of the
30 supernatant obtained from GAM medium upon HT29 and Caco2 cells was detected.
31 The sigmoid-curve fit of data obtained with HT29 allowed the calculation of different
32 toxicological parameters, such as EC50 and LOAEL values. Finally, the modification in
33 the behaviour of HT29 reordered in the RTCA was correlated with the cell rounding
34 effect, typically induced by these toxins, visualized by time-lapsed captures using an
35 optical microscope. Therefore, this RTCA method developed to test cytotoxicity
36 kinetics of *C. difficile* supernatants upon IEC could be a valuable *in vitro* model for the
37 screening of new anti-CDI agents.

38 **Key words:** *Clostridium difficile*; HT29; toxins; RTCA; RT-CES; xCELLigence

1
2
3
4
5
6
7
8
9
10
11
12
13
14
15
16
17
18
19
20
21
22
23
24
25
26
27
28
29
30
31
32
33
34
35
36
37
38
39
40
41
42
43
44
45
46
47
48
49
50
51
52
53
54
55
56
57
58
59
60
61
62
63
64
65

39 1. Introduction

40 *Clostridium difficile* is a Gram-positive, spore forming, anaerobic bacterium that
41 inhabits the large intestine of healthy individuals. However, when the intestinal
42 microbiota is disturbed (e.g. administration of oral antibiotics) this microorganism is
43 able to overgrowth leading to different pathologies, such as *C. difficile* infections (CDI)
44 in humans and animals (Rupnik et al., 2009). The main mechanism of virulence in *C.*
45 *difficile* is related to the production of the two large protein toxins TcdA (308 kDa) and
46 TcdB (260 kDa) and some variants are also able to produce the binary CDT toxin
47 (Rupnik, 2008). Both A and B toxins have the same enzymatic activity, although TcdA
48 acts mainly as enterotoxin whereas TcdB has a broad cytotoxic activity. Both toxins act
49 as glycosyltransferases inactivating host cell GTPases, then causing disruption of the
50 actin cytoskeleton and leading to colonocyte death via apoptosis; this produces a loss of
51 intestinal epithelial barrier function by opening tight junctions between cells, which
52 increased intestinal permeability and fluid accumulation, followed by the onset of
53 diarrhoea (Jank and Aktories, 2008; Voth and Ballard, 2005). Toxins also induce the
54 release of cytokines which lead to the activation of neutrophils, mast cells, enteric
55 nerves and sensory neurons within the intestinal lamina propria. These, in turn, induce
56 the release of neuropeptides and pro-inflammatory cytokines resulting in an
57 inflammatory response and pseudomembrane formation (Shen, 2012; Sun et al., 2015).

58 *C. difficile* is responsible for 20 to 30% of antibiotic-associated diarrhoea and is
59 the most frequent in nosocomial diarrhoea (Abou-Chakra et al., 2014). The CDI
60 manifestation ranges from asymptomatic carriage to clinical problems: from mild
61 diarrhoea to more severe disease syndromes, including abdominal pain, fever and
62 leucocytosis. Fulminant or severe complicated CDI is characterized by inflammatory
63 lesions and the formation of pseudomembranes in the colon, toxic megacolon or bowel

1
2
3
4
5
6
7
8
9
10
11
12
13
14
15
16
17
18
19
20
21
22
23
24
25
26
27
28
29
30
31
32
33
34
35
36
37
38
39
40
41
42
43
44
45
64 perforation, sepsis, shock and death (Faris et al., 2010). CDI have traditionally been
65 assumed to be restricted to health-care settings. However, it is known that certain
66 environments, animals and foods are predictable sources of *C. difficile*, although
67 zoonotic and foodborne transmissions have not been confirmed yet (Rodriguez-Palacios
68 et al., 2013). The main groups of risk are elders hospitalized and patients after
69 hospitalization receiving antibiotics. However, CDI is increasing in younger
70 populations, with no previous contact either with the hospital environment or with
71 antibiotics, and in specific populations that were previously considered of low risk, such
72 as children and pregnant women (Carter et al., 2012). In the recent years, the incidence
73 and mortality of CDI has significantly increased due to the emergence in North America
74 and Europe of strains with increased virulence, or hyper-virulent isolates, belonging to
75 restriction endonuclease type BI, North American pulsed-field type 1 and PCR-ribotype
76 027. In addition, emerging strains belonging to PCR-ribotype 017 and 078, which are
77 also associated with severe disease, have been isolated in parts of Asia and Europe
78 (Bouillaut et al., 2013; Drudy et al., 2007; Kim et al., 2008). Hyper-virulent strains are
79 characterized by significantly production of more A and B toxins and by their resistance
80 to fluoroquinolones; they often produce more spores, in comparison to historical strains,
81 and they synthesise the binary toxin CDT (*C. difficile* transferase) belonging to the
82 family of binary ADP-ribosylating toxins (Gerding et al., 2014; Schwan et al., 2014).

46
47
48
49
50
51
52
53
54
55
56
57
58
59
60
61
62
63
64
65
66
67
68
69
70
71
72
73
74
75
76
77
78
79
80
81
82
83
84
85
86
87
88
Therapies against CDI comprise the use of antibiotics such as metronidazole or
vancomycin, however in some cases this treatment does not prevent for the relapse of
CDI. Emerging therapeutic options are currently under investigation for treatment of
CDI (Mathur et al., 2014); in this regard, it is of pivotal relevance the use of fast,
reliable, and accurate methods allowing the screening of new potential agents against *C.*
difficile toxicity. This was the aim pursued in the current work, in which intestinal

89 cellular lines were used as biological model to follow in real time the toxic effect of a *C.*
90 *difficile* strain producing both A and B toxins.

92 **2. Material and methods**

93 **2.1. *C. difficile* culture conditions and quantification of toxins**

94 [REDACTED]
95 [REDACTED]
96 [REDACTED]
97 [REDACTED]
98 [REDACTED] Both strains were
99 routinely grown (for 16 h) in [REDACTED] Clostridium Medium [RCM, Oxoid, Thermo
100 Fisher Scientific Inc., Waltham, MA] in Hungate tubes. Incubations took place at 37°C
101 under anaerobic conditions (80% N₂, 10% CO₂, 10% H₂) in a MG500 chamber (Don
102 Whitley Scientific, West Yorkshire, UK). Several broth media (Table 1, supplementary
103 Table S1) and incubation periods (24, 48, 72 and 120 h) were tested to select the best
104 conditions for survival and toxigenic activity. The OD (600 nm), pH and counts, made
105 in each corresponding medium supplemented with 2% agar, were measured to follow *C.*
106 *difficile* activity. [REDACTED]

107 [REDACTED]
108 [REDACTED]
109 [REDACTED]
110 [REDACTED].

111 The concentration of A and B toxins produced by *C. difficile* LMG21717
112 [REDACTED] was determined by independent ELISA tests (tgcBIOMICS GmbH, Bingen,
113 Germany) following the manufacturer's instructions.

114

115 **2.2. Cell-line cultures**

116 The intestinal epithelial cell (IEC) lines HT29 (ECACC 91072201) and Caco2 (ECACC
117 86010202) were purchased from the “European Collection of Cell Cultures” (Salisbury,
118 UK) and stored at IPLA under liquid N₂. Both cell lines were maintained under standard
119 conditions using two specific media: supplemented McCoy’s medium (or MM), for
120 HT29, and supplemented Dulbecco’s modified Eagle medium (or DMEM), for Caco2
121 (Hidalgo-Cantabrana et al., 2014). Both media were added, as well, with a mixture of
122 antibiotics (50 µg/ml streptomycin-penicillin, 50 µg/ml gentamicin and 1.25 µg/ml
123 [REDACTED] B). All media and reagents were purchased from Sigma-Aldrich (Sigma-
124 Aldrich Co., St. Louis, MO). For maintenance, the cell lines were incubated at 37°C,
125 5% CO₂ atmosphere in a CO₂-Series Shel-Lab incubator (Sheldon Manufacturing Inc.,
126 OR, USA) and were weekly trypsinized. A few consecutive passages were used: from
127 p146 to p148, for HT29, and from p47 to p48, for Caco2. Cells were grown in 25 cm²
128 bottles with vented (0.2 µm membrane) cap (Falcon®, Corning Inc. Life Science,
129 Tewksbury, MA) and after 5 or 7 days of incubation these cultures were used to harvest
130 cells for the real time experiments.

131

132 **2.3. Monitoring cell-line behaviour in real-time**

133 The RTCA (real time cell analyser) xCELLigence equipment (ACEA Bioscience Inc.,
134 San Diego, CA), which monitors three independent 16-well E-plates ([REDACTED]
135 [REDACTED]), was used to test the behaviour of the IEC
136 (Hidalgo-Cantabrana et al., 2014). The equipment was introduced in a Heracell-240
137 Incubator (Thermo Electron LDD GmbH, Langenselbold, Germany), set at 37°C with
138 5% CO₂ atmosphere, and it was connected with a computer that controls and records the

1
2
3
4
5
6
7
8
9
10
11
12
13
14
15
16
17
18
19
20
21
22
23
24
25
26
27
28
29
30
31
32
33
34
35
36
37
38
39
40
41
42
43
44
45
46
47
48
49
50
51
52
53
54
55
56
57
58
59
60
61
62
63
64
65

139 RTCA-curves. Initially, both IEC were titrated to determine the number of cells needed
140 for further experiments. A cell suspension (1×10^6 cell/ml) was made in the
141 corresponding medium for each IEC and, afterwards, serial $\frac{1}{2}$ dilutions were prepared.
142 Finally, 200 μ l of the different cell suspensions were seed, in duplicated wells, in two
143 independent 16-well E-plates (Fig. 1A). These micro-plates were hold in the equipment
144 and incubated at 37°C, 5% CO₂ to record the cell index (CI) every 15 min, for 50 h. The
145 CI is an arbitrary unit that indicates variations of the impedance in gold-
146 microelectrodes, placed in the bottom of the E-plates, as consequence of the IEC
147 attachment and growth as well as due to morphological changes.

148

149 **2.4. Monitoring the cytotoxic effect of *C. difficile* upon IEC**

150 To analyse the cytotoxic effect of *C. difficile* LMG21717 both IEC were used in
151 confluent (monolayer) state and the standard working parameters were defined
152 accordingly to the titration results (Fig. 1B). An initial number of 2×10^5 cells (in 100 μ l)
153 were seed per well, thus allowing the formation of a monolayer around 14-15 h post-
154 seeding. After 7-8 h of post-confluent state (around 22 h of total incubation) culture
155 medium was removed; then different *C. difficile* samples (in 200 μ l) were added and the
156 monitoring continued (every 10 min) for additional 23 ± 1 h under the standard
157 incubation conditions. The duration of a typical experiment was 44 h, which ends with
158 the data analysis carried out with the RTCA software 1.2.1 (ACEA Bioscience).

159

160

161

162

163

164

165

166

167

168

169 **2.5. Image monitoring in real-time conditions**

170 The compact, inverted, optical microscope LumaScope-600 Series (Etaluma, Carlsbad,
171 CA) with a 40x objective was used to visualize, in time-lapsed capture images, the toxic
172 effect of *C. difficile* samples under culturing conditions. For that purpose, the
173 microscope was introduced in the Heracell-240 Incubator and was connected with an
174 external computer that captures the images, every 10 min, by means of the
175 LumaView600Cy 13.7.17.0 software (Etaluma). An optical quality (equivalent to
176 coverslip no. 1.5), standard bottom μ -Slide 2-well plate (Ibidi GmbH, Martinsried,
177 Germany) was used to monitor the formation of the HT29 monolayer after initially
178 seeding 1 ml of 2×10^6 cells/ml suspension (). Once that the confluent state was
179 reached, and at the time defined with the RTCA-DP equipment (~22 h), MM
180 supplemented with 2.5% *C. difficile* supernatant (collected from 48 h cultures in GAM)
181 was added and the image capture continued for additional 24 h.

182

183 **2.6. Statistical analysis**

184 The statistical package IBM SPSS Statistics for Window Version 22.0 (IBM Corp.,
185 Armonk NY) was used to asses differences in response (normalized CI) of HT29 due to
186 the supernatant dose by means of one-way ANOVA test. Afterwards, differences among
187 doses were determined by the Duncan mean comparison test which allowed identifying
188 the LOAEL (lowest observed adverse effect level) and NOAEL (non-observed adverse

189 effect level) doses (Jeffery et al., 2004). Finally, the EC50 (concentration at which the
190 half of the maximum adverse effect was detected) at a defined time point was calculated
191 by the RTCA software 1.2.1 (ACEA Bioscience) from the normalized-CI vs. log
192 concentration data fitted to a sigmoidal-curve.

193

194 **3. Results**

195 **3.1. *C. difficile* [REDACTED] cultures in GAM has the highest toxic effect upon HT29**

196 The initial step to develop a method to follow in real-time the cytotoxic activity of the
197 [REDACTED] *C. difficile* [REDACTED] upon IEC was obtaining a toxigenic supernatant. For that
198 purpose, eight different media and four sampling points were screened. [REDACTED]

199 [REDACTED]

200 [REDACTED] In the remaining media, the
201 highest counts ($>1 \times 10^7$ CFU/ml) were reached at this incubation period, whilst longer
202 periods led to a reduction in the bacterial counts (data no shown). To test the toxigenic
203 capability of *C. difficile*, the behaviour of HT29 in presence of 20% supernatants (Fig.
204 2A) or pellets (Fig. 2B) collected from the cultures in different media and incubation
205 periods, was monitored in real-time. The CI values obtained were normalized by the
206 control sample (MM without *C. difficile* factors) and by the time at which the factors
207 were added. The lowest normalized-CI value indicates the highest toxigenic capability
208 of *C. difficile* factors upon HT29 since the reduction of this unit reflects the detachment
209 of the cell line, from the gold-microelectrode in the E-plate, or modifications in the
210 morphology of the cell-line monolayer. For practical purposes, we have arbitrary set the
211 point of 4-h after factor addition, to obtain numeric values allowing comparisons among
212 factors (Table 2). In agreement with the absence of growth, both supernatants and
213 pellets collected from 48-h cultures in RCM, BHI-C, BHI-Suppl, or BHI-C-FSB

1
2
3
4
5
6
7
8
9
10
11
12
13
14
15
16
17
18
19
20
21
22
23
24
25
26
27
28
29
30
31
32
33
34
35
36
37
38
39
40
41
42
43
44
45
46
47
48
49
50
51
52
53
54
55
56
57
58
59
60
61
62
63
64
65

214 showed the highest normalized CI values along all monitored period (Fig. 2A and B) or
215 at the defined 4-h point (Table 2). Remarkably, the pellet harvested from BHI medium
216 retained all toxigenic activity, since its corresponding supernatant showed a normalized-
217 CI near zero. An intermediate pattern was denoted for *C. difficile* grown in
218 RCM+BHI+FSB given that produced the most toxigenic pellet, but being able to release
219 part of the toxins to the supernatant. Finally, the two media containing GAM produced
220 the more toxic supernatants and also their corresponding pellets showed low
221 normalized-CI values, i.e. high toxicity. In order to be able to choose one of these two
222 GAM media, the normalized-CI after 4-h was calculated for both factors harvested from
223 grown cultures after 72 and 120 h of *C. difficile* incubation. The supernatant collected
224 from GAM, without supplementation, showed the highest toxigenic capability which
225 remained stable during prolonged *C. difficile* culturing periods (Fig. 2C). Therefore, as
226 conditions to obtain toxigenic supernatants for further experiments we have selected
227 cultivation of *C. difficile* LMG21717 in GAM medium for 48 h. The concentration of
228 toxin A and toxin B quantified under these conditions was 210±51 ng/ml and 16±8
229 ng/ml, respectively. The supernatant collected from these culture conditions was stored
230 at -80°C until its use, since we have detected that higher temperature (-20°C) of storage
231 reduced the activity of the supernatants (data no shown).

232

233 **3.2. *C. difficile* toxic effect is dose dependent**

234 Next, we aimed at determining whether the toxigenic effect was dependent on the
235 amount of supernatant added and if was maintained during prolonged periods. To
236 achieve this goal experiments upon HT29 monolayers were performed using a wide
237 supernatant-percentage range. Immediately after the supernatant addition, it is
238 noticeable the increase in the impedance (CI) signal, which it can be easily followed in

1
2
3
4
5
6
7
8
9
10
11
12
13
14
15
16
17
18
19
20
21
22
23
24
25
26
27
28
29
30
31
32
33
34
35
36
37
38
39
40
41
42
43
44
45
46
47
48
49
50
51
52
53
54
55
56
57
58
59
60
61
62
63
64
65

239 the normalized-CI graphic (Fig. ■■■). The maximum normalized-CI values are reached
240 around 45 min after supernatant addition, the highest being at the highest doses (CI >
241 0.05 for concentrations above 2.5%). This behaviour is related with changes in the
242 morphology and shape of the eukaryotic cells. Afterwards, the CI signal showed a
243 continuous reduction over time and after 2 h, the CI recorded for most concentrations
244 tested started to show negative values. The normalized-CI drop was more drastic at
245 higher supernatant concentrations, as indicated the higher slopes obtained in the
246 normalized-CI vs. time curves. This behaviour suggests a ■■■ in the monolayer
247 integrity, which could be due to a disruption of the tight junctions between adjacent
248 cells, to cellular death, or to a combination of both events. The sigmoid-curve fit ($R^2 =$
249 0.9941) of normalized-CI vs. log concentration (percentages) obtained 4-h after
250 supernatants addition, clearly demonstrated the toxigenic dose-dependent effect of the
251 *C. difficile* supernatant upon HT29 monolayers (Fig. ■■■). Using this fit the LOAEL, i.e.
252 the lowest concentration of *C. difficile* supernatants that produced a detectable toxic
253 effect ($p < 0.05$), was 0.0781% which corresponded to 164 and 12.5 pg/ml of TcdA and
254 TcdB, respectively. Therefore, the NOAEL, or the highest concentration of supernatant
255 tested that causes no toxic effect, was 0.0391% (390.8 ppm). The concentration
256 inducing half of the maximum effect (EC50 dose) was 0.6206% (1304 and 99 pg/ml for
257 TcdA and TcdB, respectively). After longer periods of co-incubation (22-h) the
258 different doses of *C. difficile* supernatants still had a stronger toxigenic effect upon
259 HT29 cells, as the lower normalized-CI values reached indicates (Table 3). ■■■

260 ■■■

261 ■■■

262 ■■■

263 ■■■

264

265

266

267

268

269

270

271

272

273

274

275

276

277

278

279

280

281

282

283 **3.3. Visualization of *C. difficile* toxic effect**

284

285

286

287

288

In a step further, we want to assess whether results obtained with [REDACTED] [REDACTED] could be reproduced in another biological model. In this regard, Caco2 and HT29 cell lines have extensively being used in research to mimic the human intestinal epithelium. Under confluent and differentiated state both cell lines express characteristic of enterocytes, but Caco2 monolayers are composed exclusively of absorptive cells, whilst HT29 also includes mucus-secretory Goblet cells (Hilgendorf et al., 2000). Then in our study the IEC line Caco2 was confronted with the *C. difficile* toxigenic supernatant in percentages ranging from 10% to 0.16% (Fig. 4). Indeed, although we have observed a toxigenic effect of the *C. difficile* supernatant upon Caco2 monolayers, the normalized-CI values showed a different tendency with respect to that of HT29. After a short 4-h contact period, only concentrations of *C. difficile* supernatants higher than 1.25% were toxic; this cut-off percentage went down to 0.63% for prolonged co-incubation period (Table 3). Therefore, the intrinsic characteristics of each IEC accounted for the development of a model to address the toxigenic effect of this pathogen.

1
2
3
4
5
6
7
8
9
10
11
12
13
14
15
16
17
18
19
20
21
22
23
24
25
26
27
28
29
30
31
32
33
34
35
36
37
38
39
40
41
42
43
44
45
46
47
48
49
50
51
52
53
54
55
56
57
58
59
60
61
62
63
64
65

289 indicating that tight junctions and cytoskeleton are intact. In a short period after
290 supernatant addition, around 2 h, the cells into the monolayer become to acquire a
291 spherical shape and tend to detach from the adjacent ones. This is in agreement with the
292 way of action of the toxins which disarray actin cytoskeleton and finally induce cell
293 death.

294

295 **4. Discussion**

296 Treatment for CDI involves the use of antibiotics to eliminate the pathogen or, more
297 recently, the restoration of the intestinal microbiota to avoid relapse (van Nood et al.,
298 2013) which is still a controversial issue limiting its widespread use. Novel, -alternative
299 to antibiotics-, antimicrobial strategies towards *C. difficile* are currently under
300 evaluation; for example, the use of other microbial-origin molecules such as
301 bacteriocins (Gebhart et al., 2015) and bacteriophage endolysins (Dunne et al., 2014).
302 Another less explored strategy is the use of drugs targeting *C. difficile* toxins which
303 could act as co-adjuvants to palliate the acute effect induced by the pathogen (Tam et
304 al., 2015). In this article, we report the optimization of a label-free, impedance-based
305 RTCA method to follow the cytotoxicity kinetics of human colonocyte-like cells
306 exposed to *C. difficile* supernatants, method that could be used for the screening of new
307 toxin-activity inhibitors. Different label-free technologies, alternative to classic label-
308 based endpoint methods, are currently been used in different research fields such as
309 evaluation of new drugs (Xi et al., 2008) and cancer development studies (Limame et al.
310 2012), but also for assessment of the toxic effect of infectious bacteria upon host cells
311 (Slanina et al., 2011; Ye et al., 2015). Specifically the RTCA technology, also known as
312 RC-CES (real time-cell electronic sensing), was recently applied to develop methods
313 allowing the clinical diagnosis of toxigenic *C. difficile* in different biological samples

1
2
3
4
5
6
7
8
9
10
11
12
13
14
15
16
17
18
19
20
21
22
23
24
25
26
27
28
29
30
31
32
33
34
35
36
37
38
39
40
41
42
43
44
45
46
47
48
49
50
51
52
53
54
55
56
57
58
59
60
61
62
63
64
65

314 (). For this purpose cell lines from non-intestinal origin were used,
315 such as HS27 cells (fibroblast) obtained from human (Huang et al., 2014b; Ryder
316 et al., 2010), mRG1-1 cells genetically modified from CHO cells (epithelial
317 morphology) which come from Hamster ovary (He et al., 2009; Steele et al., 2012) or
318 Vero cells (epithelial morphology) obtained from a monkey kidney (Yu et al., 2015).
319 However, given that the aim pursued in our work was to develop a method allowing the
320 screening of new potential bio-actives against *C. difficile* toxicity acting within the
321 human gut, we have choose as cellular model an intestinal epithelial line since
322 enterocytes are the primary action targets of these toxins. Additionally, although the
323 results obtained with HT29 cells in proliferative state were similar (data no shown), we
324 worked in a confluent state (monolayer) because this better mimic the physiological
325 conditions of an intestinal epithelium.

326 One of the remarkable findings observed in the context of our work was the fact
327 that the culture media used to grow *C. difficile* under laboratory conditions had great
328 influence in the release (secretion) of the toxins to the supernatant. Indeed, the non-
329 selective BHI medium, classically used for growing this bacterium, retained almost all
330 toxigenic activity attached to the bacterial pellet, whereas the two media based on GAM
331 were those more effective releasing the toxins. It has been reported that culture
332 conditions, i.e. micro- and macronutrient composition, have strong influence in both
333 induction and repression of toxin production (Lei et al., 2013). In fact it was proven that
334 common rich media components, such as yeast beef and pork , are able to *in*
335 *vitro* and *in vivo* inhibit the toxicity of *C. difficile* toxin A (Duncan et al., 2009). In
336 addition, culture media also influence the composition of *C. difficile* protein secretome,
337 including their toxins (Boetzke et al. 2012). The exact mechanism of TcdA and TcdB
338 secretion is unknown

1
2
3
4
5
6
7
8
9
10
11
12
13
14
15
16
17
18
19
20
21
22
23
24
25
26
27
28
29
30
31
32
33
34
35
36
37
38
39
40
41
42
43
44
45
46
47
48
49
50
51
52
53
54
55
56
57
58
59
60
61
62
63
64
65

339 [REDACTED] such as the formation of a holin-like
340 protein, are still controversial (Govind et al., 2012; Olling et al., 2012). Therefore, to *in*
341 *vitro* evaluate the efficacy of any potential toxin's inhibitor, the laboratory *C. difficile*
342 culture conditions must be carefully chosen. In this regard, our RTCA strategy allowed
343 a fast, reliable and tailor-made method for the selection of culturing and toxin secretion
344 conditions.

345 The data of cytotoxicity kinetics obtained from the dose-response curve showed
346 an initial increase in the normalized-CI, which can be related with a modification in the
347 morphology of the cells (Hidalgo-Cantabrana et al., 2014; Yu et al., 2006), followed by
348 a drastic and continuous drop of this value during prolonged incubation times.
349 Additionally, a strong dose-response behavior was detected with a good fit ($R^2 > 0.99$) to
350 a sigmoid-curve allowing the calculation of different toxicological parameters (Jeffery
351 et al., 2014). The lowest concentration at which our model of *C. difficile* supernatants
352 induced a significantly toxic effect upon HT29 cells, after a short exposition-period (4
353 h), was 164 and 12.5 pg/ml for toxin A and B, respectively. In this regard, it has been
354 reported that TcdB is at least 100-fold more potent than TcdA upon other non-intestinal
355 cell lines (Tan et al., 2015). Thus, our data confirm this ratio upon human colonocyte-
356 like cells. As far as we could achieve after an exhaustive literature search, there are not
357 reports about the toxicity range of *C. difficile* culture supernatants upon HT29, or
358 enterocyte-like cells, allowing comparison with the results obtained in this study.
359 Regarding other cellular models, Ryder and co-workers (2010) have also detected a
360 dose- and time-dependent effect of purified toxins upon HS27 cells, being the detection
361 limit for toxin B ~200 pg/ml with a detection time between 15 to 18 h. They also
362 succeed with the detection of toxigenic *C. difficile* in stool samples collected from 300
363 CDI patients. This assay was improved latter when an immunomagnetic separation

1
2
3
4
5
6
7
8
9
10
11
12
13
14
15
16
17
18
19
20
21
22
23
24
25
26
27
28
29
30
31
32
33
34
35
36
37
38
39
40
41
42
43
44
45
46
47
48
49
50
51
52
53
54
55
56
57
58
59
60
61
62
63
64
65

364 enrichment process was incorporated during stool preparation (Huang et al., 2014b). In
365 parallel, He and collaborators (2009) reported in mRG1-1 cells detection limits about 10
366 pg/ml and 10 ng/ml for TcdB and TcdA, respectively, after prolonged (~ 20 h)
367 incubation time.; the range of the latter decreased to 1-10 pg/ml if the assay is carried
368 out in the presence of the anti-*C. difficile* toxin A monoclonal antibody A1H3, since the
369 mRG1-1 cells were engineered to express the murine Fc gamma receptor (FcγRI)-α-
370 chain, thus increasing the sensitivity of the assay. The model develop by this group was
371 also successfully used in the detection of toxins present in blood plasma of CDI animal
372 models (Steele et al., 2012) and in two cases of human *C. difficile* toxemia (Yu et al.,
373 2015). These reports underlines that the detection limits are very dependent on the
374 cellular model used, as well as on the preparation of complex biological samples.

375 Results obtained with our RTCA cytotoxic assay were confirmed with the
376 images captured every 15-min with the time lapsed optical microscope. A time-
377 dependent cell rounding of HT29 cells was observed, which it is a typical
378 morphological change observed in different cell lines treated with *C. difficile* toxins
379 (Steele et al., 2012; May et al. 2013). This loss of shape is due to modification in the
380 cellular cytoskeleton induced by the toxins, which are able to depolymerize or
381 disassemble F-actins (May et al., 2013). Another label-free, end-point independent
382 technology to measure cellular events involves the use of a lens-free, video microscopy
383 platform (Kesavan et al., 2014). The image-monitoring in real time records similar
384 events than those measured by the impedance-based RTCA, such cell adhesion,
385 spreading, division and death. Indeed, this alternative high-throughput imaging-based
386 methodology was also used to identify new *C. difficile* TcdB inhibitors that protected
387 human (non-enterocyte) cells, in this case CHO, Vero and IMR-90, from cell rounding
388 (Tan et al., 2015).

1
2
3
4
5
6
7
8
9
10
11
12
13
14
15
16
17
18
19
20
21
22
23
24
25
26
27
28
29
30
31
32
33
34
35
36
37
38
39
40
41
42
43
44
45
46
47
48
49
50
51
52
53
54
55
56
57
58
59
60
61
62
63
64
65

389 Finally, is worth noting that the cellular model used to carry out cytotoxic
390 assays, even if the cells are from the same tissue type, had an impact ■ the results
391 obtained; we have previously observed similar findings in other types of studies using
392 different IEC lines (Hidalgo-Cantabrana et al., 2014). In relation to the aim of the
393 current work, this cell-dependent effect is especially relevant to test the efficacy of any
394 potential anti-toxin bioactive since toxicological parameters, such as EC50 or LOAEL,
395 can vary. Thus, although a broad screening can be performed with a single cell line, it
396 would be advisable the use of more than one cellular type for the definition of the
397 efficacy range of any novel candidate to inhibit *C. difficile* toxic activity.

398

399 **5. Conclusion**

400 In this work we have developed a valuable *in vitro* model to test cytotoxicity kinetics of
401 *C. difficile* supernatants upon IEC, which could be eventually used in the screening of
402 new anti-CDI agents. The model allows the preliminary selection of the appropriate
403 culture conditions, as well as the choice of the accurate doses, to undertake the further
404 toxicological assays of *C. difficile* toxins. However, it must be taken into consideration
405 the variability of the results related to the model of eukaryotic cell used to analyze
406 cytotoxicity. In addition, we consider that this model could be extended to the study of
407 other microbial cyto-toxins.

408

409 **Acknowledgements**

410 This work was financed by the FEDER European Union funds through the projects
411 AGL2012-33278 from the Spanish Ministry of Economy and Competitiveness
412 (MINECO), and EQUIP11 from the “Principado de Asturias” Regional Research Plan.
413 L. Valdés acknowledges her JAE-Pre fellowship to CSIC.

414

1
2 415 **References**
3

- 4
5 416 1. Abou-Chakra CN, Pepin J, Sirard S, Valiquette L. 2014. Risk factors for recurrence,
6
7 417 complications and mortality in *Clostridium difficile* infection: a systematic review.
8
9 418 PLoS One 9(6), e98400.
10
11 419 2. Boetzkes A, Wiebke Felkel K, Zeiser J, Jochim N, Just I, Pich A. 2012. Secretome
12
13 420 analysis of *Clostridium difficile* strains. Arch Microbiol 194, 675-687.
14
15 421 3. Bouillaut L, Self WT, Sonenshein AL. 2013. Proline-dependent regulation of
16
17 422 *Clostridium difficile* Stickland metabolism. J Bacteriol 195, 844-54.
18
19 423 4. Carter GP, Rood JI, Lyras D. 2012. The role of toxin A and toxin B in the virulence
20
21 424 of *Clostridium difficile*. Trends Microbiol 20, 21-29.
22
23 425 5. Drudy D, Harnedy N, Fanning S, Hannan M, Kyne L. 2007. Emergence and control
24
25 426 of fluoroquinolone-resistant, toxin A-negative, toxin B-positive *Clostridium*
26
27 427 *difficile*. Infect Control Hosp Epidemiol 28, 932-940.
28
29 428 6. Duncan PI, Fotopoulos G, Pasche E, Porta N, Elmelegy IM, Sanchez-Garcia JL,
30
31 429 Bergonzelli GE, Corthésy-Theulaz I. 2009. Yeast, beef and pork extracts counteract
32
33 430 *Clostridium difficile* toxin A enterotoxicity. FEMS Microbiol Lett 295, 218-225.
34
35 431 7. Dunne M, Mertens HDT, Garefalaki V, Jeffries CM, Thompson A, Lemke EA,
36
37 432 Svergun DI, Mayer MJ, Narbad A, Meijers R. 2014. The CD27L and CTP1L
38
39 433 endolysins targeting Clostridia contain a built-in trigger and release factor. PLoS
40
41 434 Pathog 10(7), e1004228.
42
43 435 8. Faris B, Blackmore A, Haboubi N. 2010. Review of medical and surgical
44
45 436 management of *Clostridium difficile* infection. Tech Coloproctol 14, 97-105.
46
47 437 9. Gebhart D, Lok S, Clare S, Tomas M, Stares M, Scholl D, Donskey CJ, Lawley TD,
48
49 438 Govonia GR. 2015. A modified R-Type bacteriocin specifically targeting
50
51
52
53
54
55
56
57
58
59
60
61
62
63
64
65

1
2
3
4
5
6
7
8
9
10
11
12
13
14
15
16
17
18
19
20
21
22
23
24
25
26
27
28
29
30
31
32
33
34
35
36
37
38
39
40
41
42
43
44
45
46
47
48
49
50
51
52
53
54
55
56
57
58
59
60
61
62
63
64
65

439 *Clostridium difficile* prevents colonization of mice without affecting gut microbiota
440 diversity. mBio 6(2), e02368.

441 10. Gerding DN, Johnson S, Rupnik M, Aktories K. 2014. *Clostridium difficile* binary
442 toxin CDT: mechanism, epidemiology, and potential clinical importance. Gut
443 Microbes 5, 15-57.

444 11. Govind R, Dupuy B. 2012. Secretion of *Clostridium difficile* toxins A and B
445 requires the holin-like protein TcdE. PLoS Pathog 8(6), e1002727.

446 12. He X, Wang J, Steele J, Sun X, Nie W, Tzipori S, Feng H. 2009. An ultrasensitive
447 rapid immunocytotoxicity assay for detecting *Clostridium difficile* toxins. J
448 Microbiol Meth 78, 97-100.

449 13. Hidalgo-Cantabrana C, Kekkonen R, de los Reyes-Gavilán CG, Salminen S,
450 Korpeta R, Gueimonde M, Ruas-Madiedo P. 2014. Effect of bacteria used in food
451 industry on the proliferation and cytokine production. J Funct Foods 6, 348-355.

452 14. Hilgendorf C, Spahn-Langguth H, Regardh CG, Lipka E, Amidon GL, Langguth P.
453 2000. Caco-2 versus Caco-2/HT29-MTX co-cultured cell lines: permeabilities via
454 diffusion, inside- and outside-directed carrier-mediated transport. J Pharm Sci 89,
455 63-75.

456 15. Huang B, Li H, Jin D, Stratton CW, Tang YW. 2014a. Real-time cellular analysis
457 for quantitative detection of functional *Clostridium difficile* toxin in stool. Expert
458 Rev Mol Diagn 14, 281-291.

459 16. Huang B, Jin D, Zhang J, Sun JY, Wang X, Stiles J, Xu X, Kamboj M, Babady NE,
460 Tang YW. 2014b. Real-time cellular analysis coupled with a specimen enrichment
461 accurately detects and quantifies *Clostridium difficile* toxins in stool. J Clin
462 Microbiol 52, 1105-1111.

- 1
2
3
4
5
6
7
8
9
10
11
12
13
14
15
16
17
18
19
20
21
22
23
24
25
26
27
28
29
30
31
32
33
34
35
36
37
38
39
40
41
42
43
44
45
46
47
48
49
50
51
52
53
54
55
56
57
58
59
60
61
62
63
64
65
- 463 17. Jank T, Aktories K. 2008. Structure and mode of action of clostridial glucosylating
464 toxins: the ABCD model. Trends Microbiol 16, 222-229.
- 465 18. Jeffery B, Barlow t, Moizer K, Paul S, Boyle C. 2004. Amnesic shellfish poison.
466 Food Chem Toxicol 42, 545-557.
- 467 19. Kesavan SV, Momey F, Cioni O, David-Watine B, Dubrulle N, Shorte S, Sulpice E,
468 Freida D, Chalmond B, Dinten JM, Gidrol X, Allier C. 2014. High-throughput
469 monitoring of major cell functions by means of lensfree video microscopy. Sci Rep
470 4, 5942.
- 471 20. Kim H, Riley TV, Kim M, Kim CK, Yong D, Lee K, Chong Y, Park JW. 2008.
472 Increasing prevalence of Toxin A-negative, Toxin B-positive isolates of *Clostridium*
473 *difficile* in Korea: impact on laboratory giagnosis. J Clin Microbiol 46, 1116-1117.
- 474 21. Lei XH, Bochner BR. 2013. Using phenotype microarrays to determine culture
475 conditions that induce or repress toxin production by *Clostridium difficile* and other
476 microorganisms. PLoS ONE 8(2), e56545.
- 477 22. Limame1 R, Wouters A, Pauwels B, Fransen E, Peeters M, LardonF, De Wever O,
478 Pauwels P. 2012. Comparative analysis of dynamic cell viability, migration and
479 invasion assessments by novel real-time technology and classic endpoint assays.
480 PLoS ONE 7(10), e46536.
- 481 23. Mathur H, Rea MC, Cotter PD, Ross RP, Hill C. 2014. The potential for emerging
482 therapeutic options for *Clostridium difficile* infection. Gut Microbes 5, 696-710.
- 483 24. May M, Wang T, Müller M, Genth H. 2013. Difference in F-actin depolymerization
484 induced by toxin B from the *Clostridium difficile* strain VPI 10463 and toxin B from
485 the variant *Clostridium difficile* Serotype F strain 1470. Toxins 5, 106-119.

- 1
2
3
4
5
6
7
8
9
10
11
12
13
14
15
16
17
18
19
20
21
22
23
24
25
26
27
28
29
30
31
32
33
34
35
36
37
38
39
40
41
42
43
44
45
46
47
48
49
50
51
52
53
54
55
56
57
58
59
60
61
62
63
64
65
- 486 25. Olling A, Seehase S, Minton NP, Tatge H, Schröter S, Kohlscheen S, Pich A, Just I,
487 Gerhard R. 2012. Release of TcdA and TcdB from *Clostridium difficile* cdi 630 is
488 not affected by functional inactivation of the tcdE gene. *Microb Pathog* 52, 92-100.
- 489 26. Rodriguez-Palacios A, Borgmann S, Kline TR, LeJeune JT. 2013. *Clostridium*
490 *difficile* in foods and animals: history and measures to reduce exposure. *Anim*
491 *Health Res Rev* 14, 11-29.
- 492 27. Rupnik M. 2008. Heterogeneity of large clostridial toxins: importance of
493 *Clostridium difficile* toxinotypes. *FEMS Microbiol Rev* 32, 541-555.
- 494 28. Rupnik M, Wilcox MH, Gerding DN. 2009. *Clostridium difficile* infection: new
495 developments in epidemiology and pathogenesis. *Nature Rev Microbiol* 7, 526-536.
- 496 29. Ryder AB, Huang Y, Li H, Zheng M, Wang X, Stratton CW, Xu X, Tang YW.
497 2010. Assessment of *Clostridium difficile* infections by quantitative detection of
498 TcdB toxin by use of a real-time cell analysis System. *J Clin Microbiol* 48, 4129-
499 4164.
- 500 30. Schwan C, Kruppke AS, Nölke T, Schumacher L, Koch-Nolte F, Kudryashev M,
501 Stahlberg H, Aktories K. 2014. *Clostridium difficile* toxin CDT hijacks microtubule
502 organization and reroutes vesicle traffic to increase pathogen adherence. *Proc Natl*
503 *Acad Sci U S A* 111, 2313-2318.
- 504 31. Shen A. 2012. *Clostridium difficile* toxins: mediators of inflammation. *J Innate*
505 *Immun* 4, 149-158.
- 506 32. Slanina H, König A, Claus H, Frosch M, Schubert-Unkmeir A. 2011. Real-time
507 impedance analysis of host cell response to meningococcal infection. *J Microbiol*
508 *Meth* 84, 101-108.

1
2
3
4
5
6
7
8
9
10
11
12
13
14
15
16
17
18
19
20
21
22
23
24
25
26
27
28
29
30
31
32
33
34
35
36
37
38
39
40
41
42
43
44
45
46
47
48
49
50
51
52
53
54
55
56
57
58
59
60
61
62
63
64
65

509 33. Steele J, Chen K, Sun X, Zhang Y, Wang H, Tzipori S, Feng H. 2012. Systemic
510 dissemination of *Clostridium difficile* toxins A and B is associated with severe, fatal
511 disease in animal models. J Infect Dis 205, 384-391.

512 34. Sun X, Hirota SA. 2015. The roles of host and pathogen factors and the innate
513 immune response in the pathogenesis of *Clostridium difficile* infection. Mol
514 Immunol 63, 193-202.

515 35. Tam J, Beilhartz GL, Auger A, Gupta P, Therien AG, Melnyk RA. 2015. Small
516 molecule inhibitors of *Clostridium difficile* toxin B-induced cellular damage. Chem
517 Biol 22, 175-185.

518 36. van Nood E, Vrieze A, Nieuwdorp M, Fuentes S, Zoetendal EG, de Vos WM,
519 Visser CE, Kuijper EJ, Bartelsman JFWM, Tijssen JGP, Speelman P, Dijkgraaf
520 MGW, Keller JJ. 2013. Duodenal infusion of donor feces for recurrent *Clostridium*
521 *difficile*. N Engl J Med 368, 407-415.

522 37. Voth DE, Ballard JD. 2005. *Clostridium difficile* toxins: mechanism of action and
523 role in disease. Clin Microbiol Rev 18, 247-263.

524 38. Xi B, Yu N, Wang X, Xu X, Abassi YA. 2008. The application of cell-based label-
525 free technology in drug discovery. Biotechnol J 3, 484-495.

526 39. Ye J, Luo Y, Fang W, Pan J, Zhang Z, Zhang Y, Chen Z, Jin D. 2015. Real-time cell
527 analysis for monitoring cholera toxin-induced human intestinal epithelial cell
528 response. Curr Microbiol 70, 536-543.

529 40. Yu N, Atienza JM, Bernard J, Blanc S, Zhu J, Wang X, Xu X, Abassi YA. 2006.
530 Real-time monitoring of morphological changes in living cells by electronic cell
531 sensor arrays: an approach to study G protein-coupled receptors. Anal Chem 78, 35-
532 43.

1
2
3
4
5
6
7
8
9
10
11
12
13
14
15
16
17
18
19
20
21
22
23
24
25
26
27
28
29
30
31
32
33
34
35
36
37
38
39
40
41
42
43
44
45
46
47
48
49
50
51
52
53
54
55
56
57
58
59
60
61
62
63
64
65

533 41. Yu H, Chen K, Wu J, Yang Z, Shi L, Barlow LL, Aronoff DM, Garey KW, Savidge
534 TC, von Rosenvinge EC, Kelly CP, Feng H. 2015. Identification of toxemia in
535 patients with *Clostridium difficile* infection. PLoS ONE 10(4), e0124235.

536

537 **Table 1.** Composition of culture media used to select the best conditions for growth and
 538 toxin production of *Clostridium difficile* LMG21717.

Medium	Composition	Brands ¹
RCM	(supplementary table S1)	Oxoid
BHI	(supplementary table S1)	Oxoid
GAM	(supplementary table S1)	Nissui
RCM+BHI+FSB	1 vol RCM + 1 vol BHI + Foetal Serum Bovine (5%)	Oxoid, Sigma
BHI-C	BHI + L-cysteine (0.25%)	Oxoid, Sigma
BHI-Suppl.	BHI + L-cysteine (0.25%) + yeast extract (0.5%) + sodium thioglycolate (0.1%)	Oxoid, BD-Difco, Sigma
BHI-C-FSB	BHI + L-cysteine (0.25%) + Foetal Serum Bovine (5%)	Oxoid, Sigma
GAM-FSB	GAM + Foetal Serum Bovine (5%)	Nissui, Sigma

539 ¹ Oxoid, Thermo Fisher Scientific Inc., Waltham, MA; Nissui Pharmaceutical Co., Ltd., Tokyo, Japan;
 540 Sigma-Aldrich Co., St. Louis, MO; BD-Difco, Becton Dickinson Co., Franklin Lakes, NJ.

541

542 **Table 2** Cultures of *Clostridium difficile* LMG21717, after 48 h of incubation, made in
 543 different media used to select the best conditions for growth and toxigenic activity. The
 544 highest toxigenic activity was established at the lowest normalized-cell index (CI) value
 545 obtained from the intestinal cell lines HT29 and Caco2 after 4 h of *C. difficile* factors
 546 addition.

Media	<i>C. difficile</i>			Normalized-CI HT29	
	pH	OD	CFU/ml	Supernatant	Pellet
RCM	5.62	1.26	< 10 ⁵	-0.0191	-0.0793
BHI	5.88	1.10	8.3x10 ⁷	-0.0912	-0.6199
RCM+BHI+FSB	5.64	1.66	1.1x10 ⁷	-0.3077	-0.7109
GAM	5.88	1.25	1.6x10 ⁷	-0.7052	-0.5211
BHI-C	5.47	1.52	< 10 ⁵	-0.0566	-0.1958
BHI-Suppl.	5.51	1.72	< 10 ⁵	-0.1069	-0.2708
BHI-C-FSB	5.50	1.24	< 10 ⁵	-0.0739	-0.1721
GAM-FSB	5.84	1.64	1.4x10 ⁷	-0.7267	-0.6820

547

548

549 **Table 3** Normalized-cell index (CI) values obtained from the intestinal cell lines HT29
 550 and Caco2 after 4 h and 22 h of addition of different concentrations of *Clostridium*
 551 *difficile* LMG21717 toxigenic supernatants.

<i>C. difficile</i> supernatant	Normalized-CI			
	HT29		Caco2	
	4 h	22 h	4 h	22 h
10%	-0.6253	-0.8468	-0.2741	-0.6662
5%	-0.5665	-0.8228	-0.2596	-0.6427
2.5%	-0.4935	-0.7956	-0.1151	-0.6367
1.25%	-0.4125	-0.7728	0.0191	-0.6135
0.63%	-0.3262	-0.7303	0.0576	-0.4668
0.31%	-0.2301	-0.6923	0.0048	0.0279
0.16%	-0.1604	-0.6198	-0.0756	0.1079
0 (control)	0	0	0	0

552



553

1
2
3
4
5
6
7
8
9
10
11
12
13
14
15
16
17
18
19
20
21
22
23
24
25
26
27
28
29
30
31
32
33
34
35
36
37
38
39
40
41
42
43
44
45
46
47
48
49
50
51
52
53
54
55
56
57
58
59
60
61
62
63
64
65

554 **Figure legend**

555 **FIG. 1** Titration of HT29 and Caco2 cells dependent on the initial number of cells
556 seeded (A). Experimental design used to test the toxic effect of *C. difficile* LMG21717
557 (B) and microscopic visualization of the HT29 cell morphology immediately after
558 seeding (left microphotograph) and when the confluent monolayer state was reached
559 (right microphotograph).

560
561 **FIG. 2** Behaviour of HT29 monolayers in the presence of the toxigenic supernatants
562 and pellets collected from *C. difficile* cultures grown for 48 h in different culture media.
563 Normalized cell index (CI) obtained from E-plates to test McCoy's medium
564 supplemented with 20% of supernatants from each medium (A) or with pellets
565 resuspended (1/10 vol. of the initial 48-h culture) in McCoy's medium (B). The CI was
566 normalized by the control (non-supplemented McCoy's medium) sample at the time of
567 the supernatant or pellet addition. Normalized-CI values 4-h after addition of factors
568 obtained from 48, 72 and 120 h of *C. difficile* cultures in media containing GAM (C).

569
570 **FIG. 3** Behaviour of HT29 monolayers in the presence of different percentages of the
571 toxigenic supernatant collected from *C. difficile* cultures grown for 48 h in GAM. Mean
572 values of data after normalization of the CI by the control sample (non-supplemented
573 McCoy's medium) and by the time of the supernatant addition  Dose-response data
574 (mean and SD) fitted to a sigmoidal trend line curve allowing the identification of the
575 EC50 (concentration where supernatant produced 50% of the maximum toxic effect),
576 LOAEL (lowest observed adverse effect level, p<0.05) and NOAEL (non-observed
577 adverse effect level) doses 

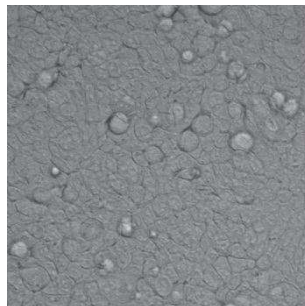
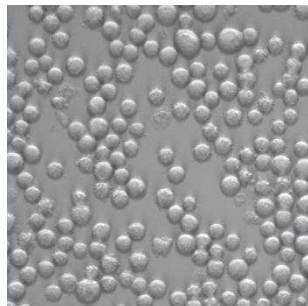
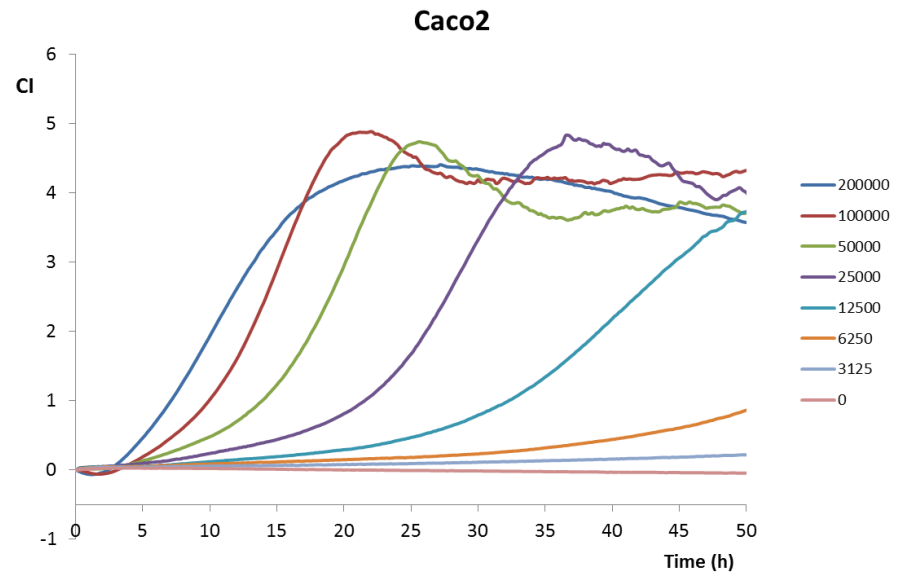
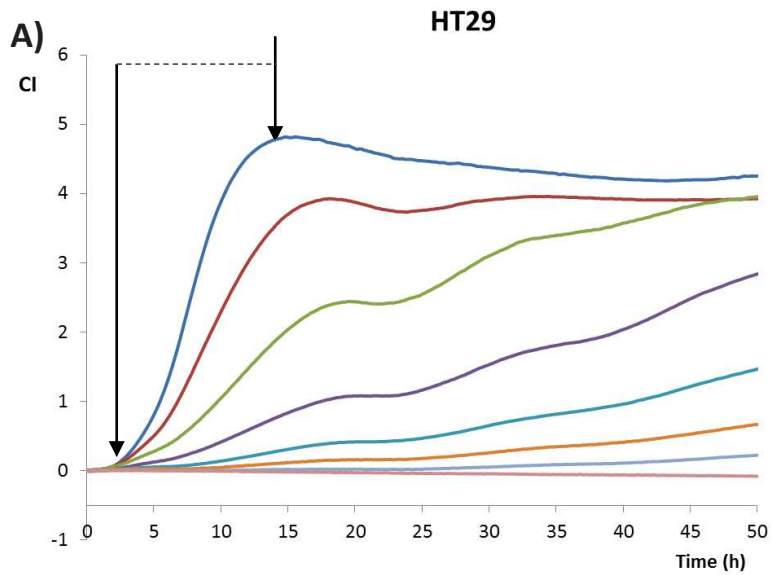
578

1
2
3
4
5
6
7
8
9
10
11
12
13
14
15
16
17
18
19
20
21
22
23
24
25
26
27
28
29
30
31
32
33
34
35
36
37
38
39
40
41
42
43
44
45
46
47
48
49
50
51
52
53
54
55
56
57
58
59
60
61
62
63
64
65

579 **FIG. 4** Behaviour of Caco2 monolayers in the presence of different percentages of the
580 toxigenic supernatant collected from *C. difficile* cultures grown for 48 h in GAM. The
581 CI was normalized by the control (non-supplemented DMEM) sample at the time of the
582 supernatant addition.

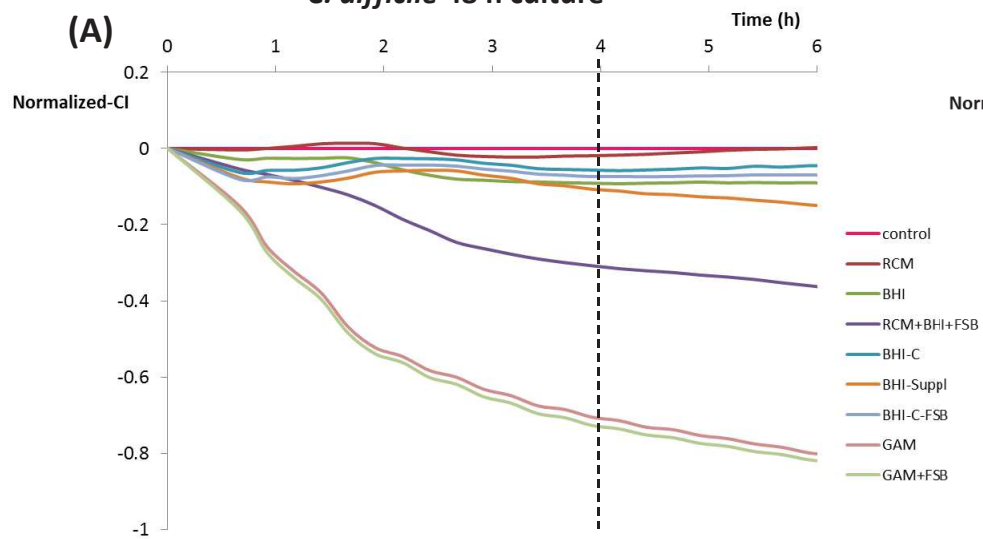
583

584 **FIG. 5** Visualization over time (from 0 to 24 h, photo-capture interval of 1h, 40 min)
585 under inverted optical microscope (objective x40) of the HT29 monolayer in the
586 presence of 2.5% *C. difficile* toxigenic supernatant collected from 48 h cultures in GAM
587 medium. Arrows indicate some areas of monolayer disaggregation. (See Supplementary
588 video, made with a selection of 100 microphotographs captured at 10 min interval, from
589 0 to 24 h).



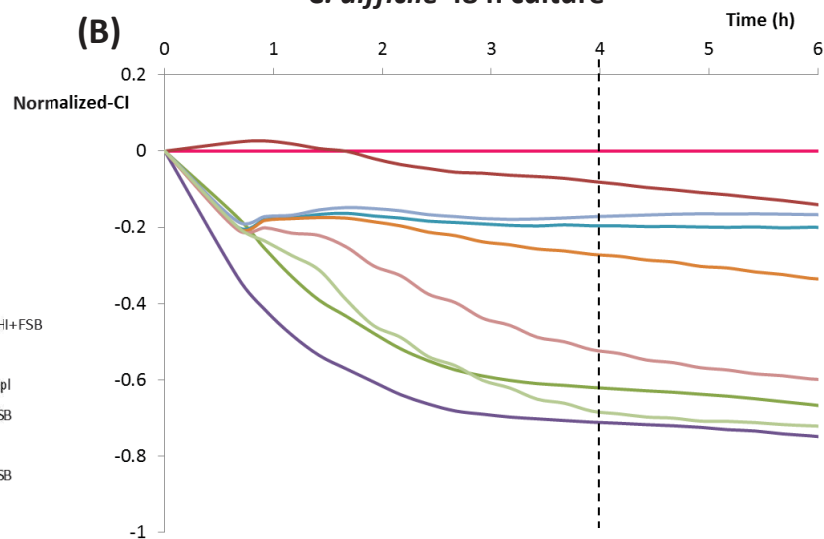
C. difficile 48 h culture

(A)

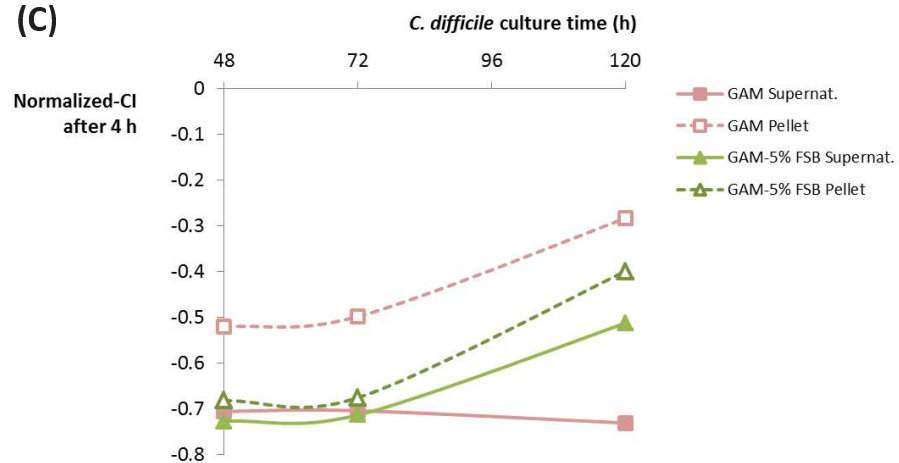


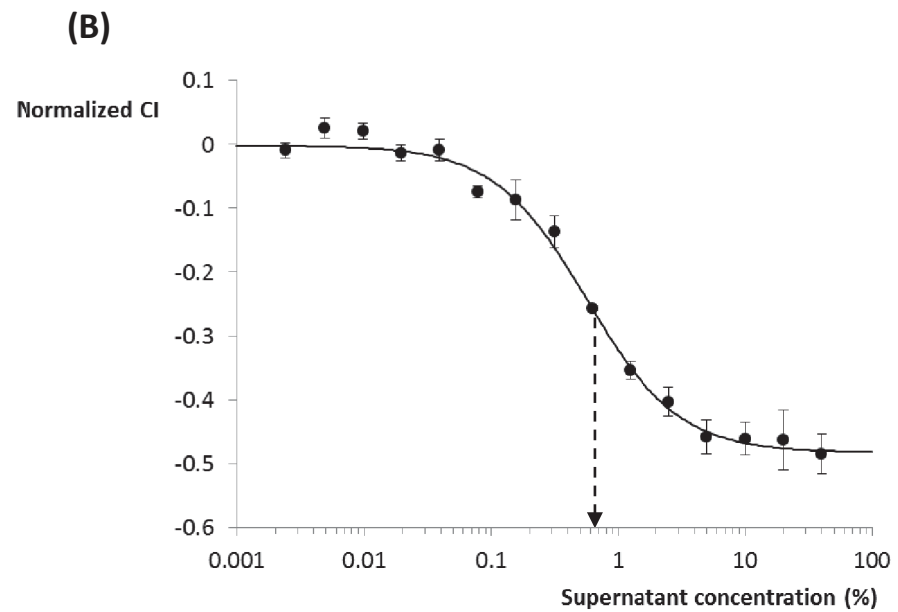
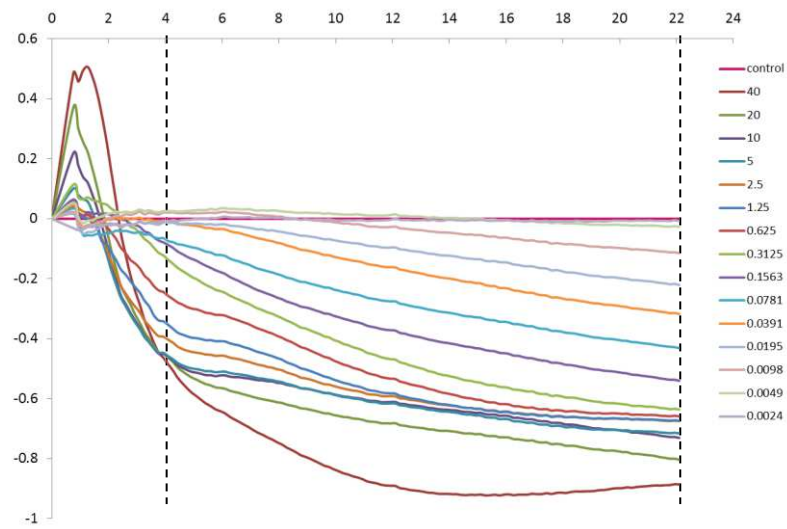
C. difficile 48 h culture

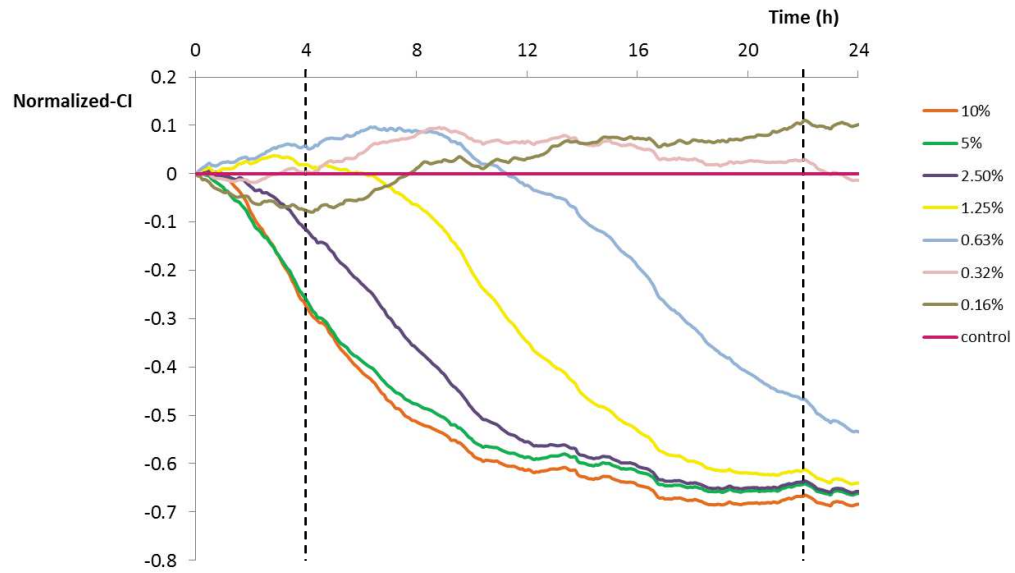
(B)

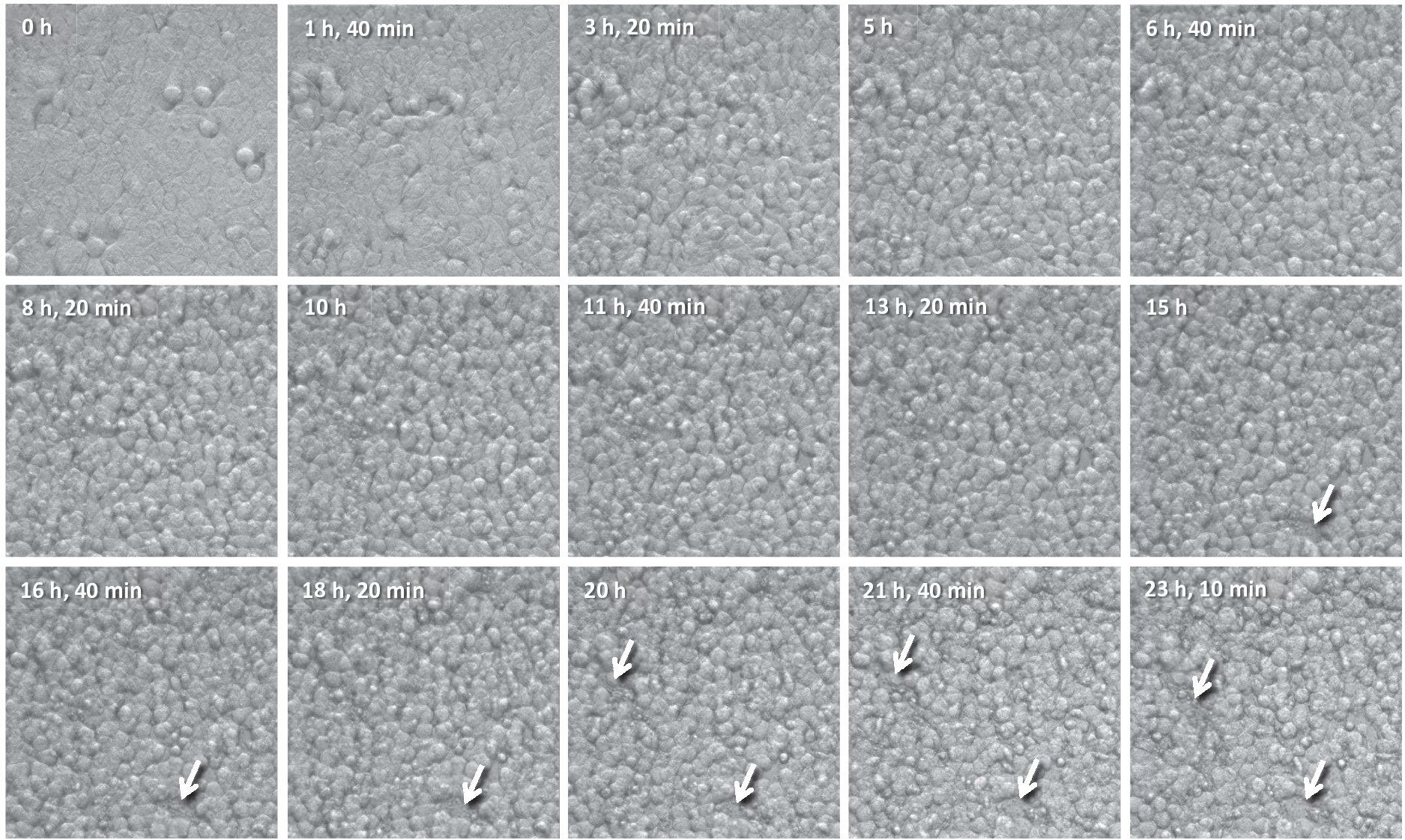


(C)









e-components

[Click here to download e-components: Supplementary material-vs2.docx](#)

Video Still

[Click here to download high resolution image](#)

